Experimental study on driftwood accumulation at submerged culverts

Ronckers, Dennis; Poppema, Daan W.; Wüthrich, Davide

DOI
10.3929/ethz-b-000676024

Publication date
2024

Document Version
Final published version

Published in
Proceedings of the 10th International Symposium on Hydraulic Structures (ISHS 2024)

Experimental study on driftwood accumulation at submerged culverts

Conference Paper

Author(s):
Ronckers, Dennis; Poppema, Daan W.; Wüthrich, Davide

Publication date:
2024

Permanent link:
https://doi.org/10.3929/ethz-b-000676024

10th International Symposium on Hydraulic Structures Zurich, Switzerland 17-19 June 2024
ISSN 0374-0056 DOI: 10.3929/ethz-b-000676024

Experimental study on driftwood accumulation at submerged culverts

Dennis Ronckers[1,2], Daan W. Poppema[1] & Davide Wüthrich[1]
[1] *Department of Hydraulic Engineering, Delft University of Technology, Delft, the Netherlands*
[2] *Province of Limburg, Maastricht, the Netherlands*
E-mail: d.w.poppema@tudelft.nl

Abstract: *This study investigates the effect of driftwood on submerged culverts through scale experiments, focusing on their accumulation and the hydrodynamic processes occurring underneath. Examining temporal evolution and velocity measurements, this research delves into the implications of driftwood accumulation, including its geometry, hydraulic conditions and associated backwater rise. Findings reveal that accumulation shape is strongly influenced by hydraulic conditions, with higher Froude numbers pulling logs toward the bottom and thus yielding more compact accumulations. This effect holds implications for submerged culverts, where the opening near the bottom diminishes the importance of surface flow resistance. Accurate prediction of accumulation lengths is achieved using wood volume and initial flow velocity. The study also provides valuable data for developing quantitative design equations for backwater rise from driftwood accumulation at culverts. Additionally, detailed measurements of velocity profiles and Reynolds stresses under the accumulations highlight a slightly lower flow velocity, prompting the need for future research to discern its generality and implications for driftwood-induced scour at submerged culverts.*

Keywords: *Driftwood, large wood, backwater rise, debris accumulation, Laser Doppler Velocimetry, carpet length*

1. INTRODUCTION

The accumulation of driftwood at critical infrastructure has often been overlooked in the realm of flood management, despite representing a critical aspect that can yield catastrophic consequences if not adequately addressed. The mishandling of strategies and an insufficient comprehension of the processes leading to large wood accumulation can significantly hamper the functionality of hydraulic structures in flood-prone areas. The 2021 floods in Belgium, Germany, and the Netherlands served as a reminder of this issue, as numerous bridges and hydraulic structures sustained severe damage due to driftwood accumulation and subsequent clogging (Korswagen et al. 2022; Erpicum et al. 2023). In the Netherlands, several culverts and inverted siphons fell victim of large driftwood accumulation, resulting in a reduced conveyance capacity and exacerbating upstream flooding (Ronckers 2023a). The village of Bunde, situated near Maastricht in the Limburg province of the Netherlands, became a prime example of this phenomenon. Large wood accumulations obstructed the entrance of an inverted syphon (Figure 1), preventing floodwaters to flow from the Geul river to the Maas, intensifying overflow along the Juliana Canal and inundating multiple nearby villages. As a consequence, additional damage was induced by the reduced capacity of these critical hydraulic structures, pointing out the need for more efficient debris management strategies.

Figure 1. Inverted siphon near Bunde (the Netherlands), affected by driftwood accumulation during the summer 2021 flood. Credit rightmost photos Waterschap Limburg.

Previous studies showed that accumulations upstream of hydraulic structures can be very heterogeneous and do not only include driftwood (*e.g.* Bayón et al. 2023; Erpicum et al. 2023). This has severe implications on the hydraulic behavior of hydraulic structures, since heterogeneous accumulations (including driftwood) were shown to induce substantially higher water levels (Honingh et al. 2020, Burghardt et al. 2024). Similar effects were also shown in coastal floods (*e.g.* tsunamis), where heterogeneous mixtures accumulate at coastal building, creating '*debris-dams*' (Wüthrich et al. 2020). Despite this, observations in Bunde revealed a predominant presence of large woody debris at inlets of this hydraulic structure, pushing this study to focus on the exclusive effect of driftwood.

Multiple previous studies have investigated the effect of driftwood (also called large wood or large woody debris) at racks and bridges, including pivotal contributions by Schmocker and Hager (2013), Schalko (2018) and Schalko et al. (2019a,b). However there exist substantial physical differences with bridges/racks, since at submerged culverts, accumulation shape and especially the location of driftwood (in front or above the culvert opening), strongly determine the degree of induced flow resistance and backwater rise. To date, there is no scientific study on the accumulation of driftwood at submerged culverts and inverted syphons, with the exception of Fu et al. (2020), who investigated the accumulation of ice upstream of inverted siphons. This pointed out a clear gap in knowledge that motivated the present research, with the aims of understanding how the presence of driftwood affects the conveyance capacity of these critical hydraulic infrastructures during extreme flood events.

2. EXPERIMENTAL SET UP

This study is based on an experimental approach and all tests were conducted in the Hydraulic Laboratory of Delft University of Technology, the Netherlands. The objective of this study was to investigate the main features associated with the accumulation of driftwood at hydraulic structures and their influence on the backwater level rise Δh, i.e. the increase in water level relative to the initial water level without driftwood h_0 (Figure 2). The physical model was built in a smooth (glass) inverted flume with a length of 14 m, a width B = 0.4 m and a height of 0.45 m, where a fully submerged outlet-controlled culvert was reproduced. Based on the dimensions of typical prototype structures in the Limburg province (*e.g.* Geul and Geleenbeek), a geometric scale of 1:20 was chosen, leading to a culvert opening δ = 0.12 m (2.4 m in the prototype) and L = 1.6 m (32 m in the prototype). The structure was made of plywood and to prevent logs from entering the culvert, a protective grid was installed on the upstream side with 4 vertical bars (⌀ = 8 mm) and a grate with openings of 4×4 mm, which was the largest size to prevent the smallest log from passing through. A movable sill was located at the end of the flume, allowing to control the water levels at the downstream end of the culvert (*i.e.* outlet control structure). Pictures of the set-up and a definition sketch with the main parameters are presented in Figure 2.

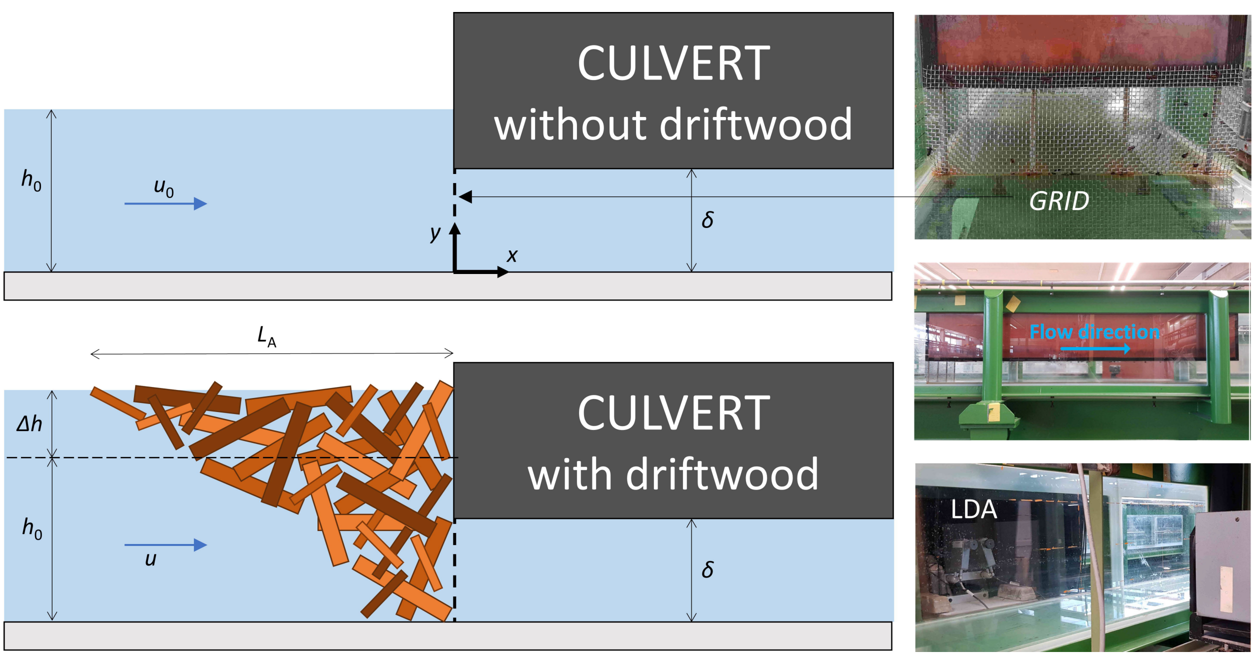

Figure 2. Definition sketch and picture of the experimental set-up, with and without driftwood.

2.1. Instrumentation

The water was conveyed into the flume from a large upper reservoir and through flow straighteners to guarantee maximum stability and good inflow conditions. The discharge was adjusted manually and measured by an ultrasonic flow meter in the supply pipeline. Water depths both upstream and downstream of the culvert were measured using point gauges with a precision of ±0.5 mm. Side-view cameras were employed to document the evolution of the large wood accumulation in front of the culvert. Flow velocities were measured using a Laser Doppler Anemometry (LDA). A cart carrying the LDA device was placed upon the rails on the sides of the flume. On one side of the flume the laser emitter was placed, and on the other side the receivers (Figure 2). Horizontal translation could be performed by moving the cart along the rails, and vertical translation by raising or lowering the frame. The system was configured such that both translations could be performed without any relative motion between the emitter and receivers. The device used a He-Ne laser with a 632.8 nm wavelength. The LDA measured the horizontal (streamwise) and vertical velocity components within an ellipsoidal volume of approximately 0.1 mm^3. The measurement frequency was set to 1,000 Hz and data was continuously collected for 3 minutes. The applicable velocity range is between 0.001 and 2 m/s, with a precision of 0.5 mm/s. The laser beams were inclined upward allowing for measurements close to the accumulation, but as a result the lowest possible measurements were approximately 25 mm above the flume bed.

2.2. Driftwood characteristics

Previous observations during the 2021 floods showed that at this specific location accumulations only contained driftwood. It was therefore decided to use a fixed volume of driftwood across all experiments with a value V_S = 7.4 L = 0.0074 m^3. Depending on the flow conditions in Table 1, this volume ranged between 0.4 to 2.3 times the characteristic value suggested by Schalko (2018). The composition of the driftwood mixture is based on observations at the Geul inverted siphon after the 2021 flood events, as documented by Ronckers (2023b). Figure 3 shows the discretised distribution of log sizes at prototype scale (laboratory was scaled 1:20). The length to diameter ratio for natural logs was assumed to be 20. The logs used in this work were natural sticks from the Limburg province, whose properties corresponded well to "*dense wood*" by Ruiz-Villanueva et al. (2014), with a buoyancy of 21% and average density of ρ_d = 800 kg/m^3.

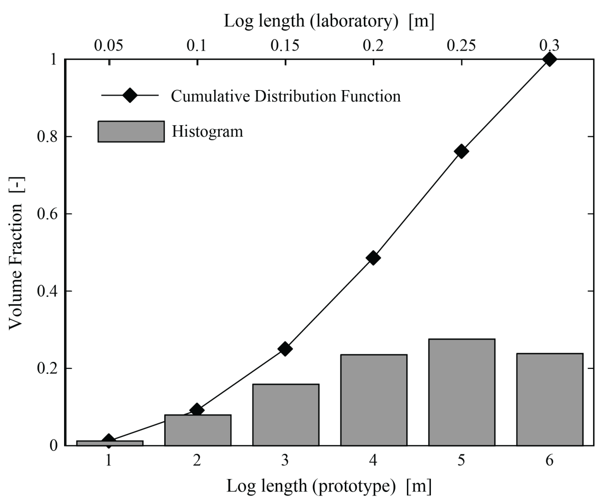

Log length [m]		**Log diameter** [cm]		N_{batch}	N_{total}
Prototype	*Lab*	*Prototype*	*Lab*		
1.0	0.05	5	0.25	33	330
2.0	0.10	10	0.50	27	270
3.0	0.15	15	0.75	16	160
4.0	0.20	20	1.00	10	100
5.0	0.25	25	1.25	6	60
6.0	0.30	30	1.50	3	30
			Total	**95**	**950**

Figure 3. Driftwood characteristics. Note that an additional 10% was included in V_S = 7.4 L (lab scale) to consider irregularities in the shape of the natural logs used in this study. Both prototype and laboratory scale are indicated, the lab scale was 1:20.

2.3. Test procedure and experimental program

The experiments encompassed a wide range of upstream flow conditions, including the initial Froude numbers $Fr_0 = u_0/(gh_0)^{0.5}$ between 0.15 and 0.35 and different submergence rates h_0/δ (the ratio between initial flow depth and culvert height) between 1.1 and 2.0, as summarized in Table 1. The Reynolds number Re, defined as $Re = \rho u_0 h_0/\mu$, where ρ is the water density and μ the dynamic viscosity, ranged between $2.3 \cdot 10^4 < Re < 9.4 \cdot 10^4$, which was sufficiently large to guarantee a fully turbulent flow and therefore minimizing scale effects when applying a Froude scaling.

At the beginning of each test, the desired discharge was set, then the downstream sill was adjusted to reach the desired water level and submergence ratio. Careful attention was given to prevent air entrapment below the culvert. The total driftwood volume V_S was divided into 10 equal batches (Figure 3), added one at the time and therefore allowing to capture the progressive backwater rise for increasing driftwood volumes. After adding a batch of driftwood, it took about 3 minutes until the accumulation and water level reached a near-equilibrium state, after which water levels were measured and another batch of driftwood was added. Each test was repeated at least 3 times to guarantee maximum reliability. Velocity measurements were conducted for three selected flow conditions, as highlighted in Table 1. Profiles of the horizontal (streamwise) and vertical velocities were measured at the centerline of the flume, at distances of $10 \cdot \delta$ (inside the culvert), $-1 \cdot \delta$, $-2 \cdot \delta$, $-3 \cdot \delta$, $-4 \cdot \delta$, $-5 \cdot \delta$, $-10 \cdot \delta$ and $-20 \cdot \delta$. Velocity measurements were conducted from the lowest reachable point (approx. 25 mm from the bottom) to as close as possible to the driftwood accumulation, depending on the geometry of the accumulation.

Table 1. Experimental program conducted in the present study. Velocity measurements were conducted for tests in green.

Test label	Submergence h_0/δ	u_0 [m/s]	h_0 [m]	Q [L/s]	Fr_0	Re [10^4]
1A	1.10	0.17	0.132	9.0	0.15	2.3
1C	1.10	0.28	0.132	15.0	0.25	3.8
2C	1.25	0.30	0.150	18.2	0.25	4.5
2E	1.25	0.42	0.150	25.5	0.35	6.4
3A	1.40	0.19	0.168	12.9	0.15	3.2
3B	1.40	0.26	0.168	17.2	0.20	4.3
3C	1.40	0.32	0.168	21.6	0.25	5.4
3D	1.40	0.38	0.168	25.9	0.30	6.5
3E	1.40	0.45	0.168	30.2	0.35	7.5
4A	1.60	0.20	0.192	15.8	0.15	4.0
4C	1.60	0.34	0.192	26.3	0.25	6.6
4D	1.60	0.41	0.192	31.6	0.30	7.9
5C	1.80	0.36	0.216	31.4	0.25	7.9
5D	1.80	0.44	0.216	37.7	0.30	9.4
6A	2.00	0.23	0.240	22.1	0.15	5.5
6C	2.00	0.38	0.240	36.8	0.25	9.2

3. DRIFTWOOD ACCUMULATION AND CARPET FORMATION

The set-up did not allow for logs to go through the culvert, hence inducing the formation of a driftwood accumulation on the upstream side of the structure, that grew in size with the arrival of the new log batches. The pictures taken after each batch show some interesting features that are shown in Figure 4 for two selected flow conditions ($Fr_0 = 0.15$ and 0.35), both with a submergence $h_0/\delta = 1.4$. One can immediately notice a difference in behavior between $Fr_0 = 0.15$ and the higher Froude numbers, clearly showing that for weaker flows most driftwood remained floating at the surface, with a carpet that kept growing horizontally, but not vertically (*i.e.* the entrance of the culvert remains almost unblocked). This can be explained by the fact that the flow is too weak to pull many branches down towards the grate. As a result, adding more driftwood mainly increased the length of the accumulation, but the backwater rise remained limited. Contrarily, larger Froude numbers ($Fr_0 = 0.35$) showed the development of a more typical accumulation, where the flow was sufficiently strong to pull branches down towards the grate, causing substantial backwater rise. Observations also showed the accumulation to take on an arched geometry with the addition of more log batches (Figure 4), fitting with the observations of Schalko (2019a) at debris racks. The large number of logs that accumulated on the upstream side of the grate induced a drag flow through a porous medium, that is responsible for the head-losses that contribute strongly to the upstream backwater rise (Follett et al. 2020, Poppema and Wüthrich, 2024). Similar results were observed for other flow conditions and submergence rates, as detailed by Ronckers (2023a).

A particularly relevant parameter for engineers and designers is the length of the accumulation L_A, defined as the horizontal distance between the most upstream log and the inlet of the culvert (Figure 2). This value was measured 3 minutes after each batch was introduced in the flume and its development is depicted in Figure 5, as a function of the initial velocity u_0 and of which fraction of the total volume V_S is added. Results showed, as expected, that the length of the accumulation grew for increasing driftwood volumes. A correlation between the accumulation length and u_0 is also clearly visible: higher values of u_0 generate shorter accumulations. Images also confirm that higher initial velocities u_0 can drag logs to the entrance of the culvert, therefore increasing the local head losses and inducing higher backwater level rises, as previously shown in Figure 4.

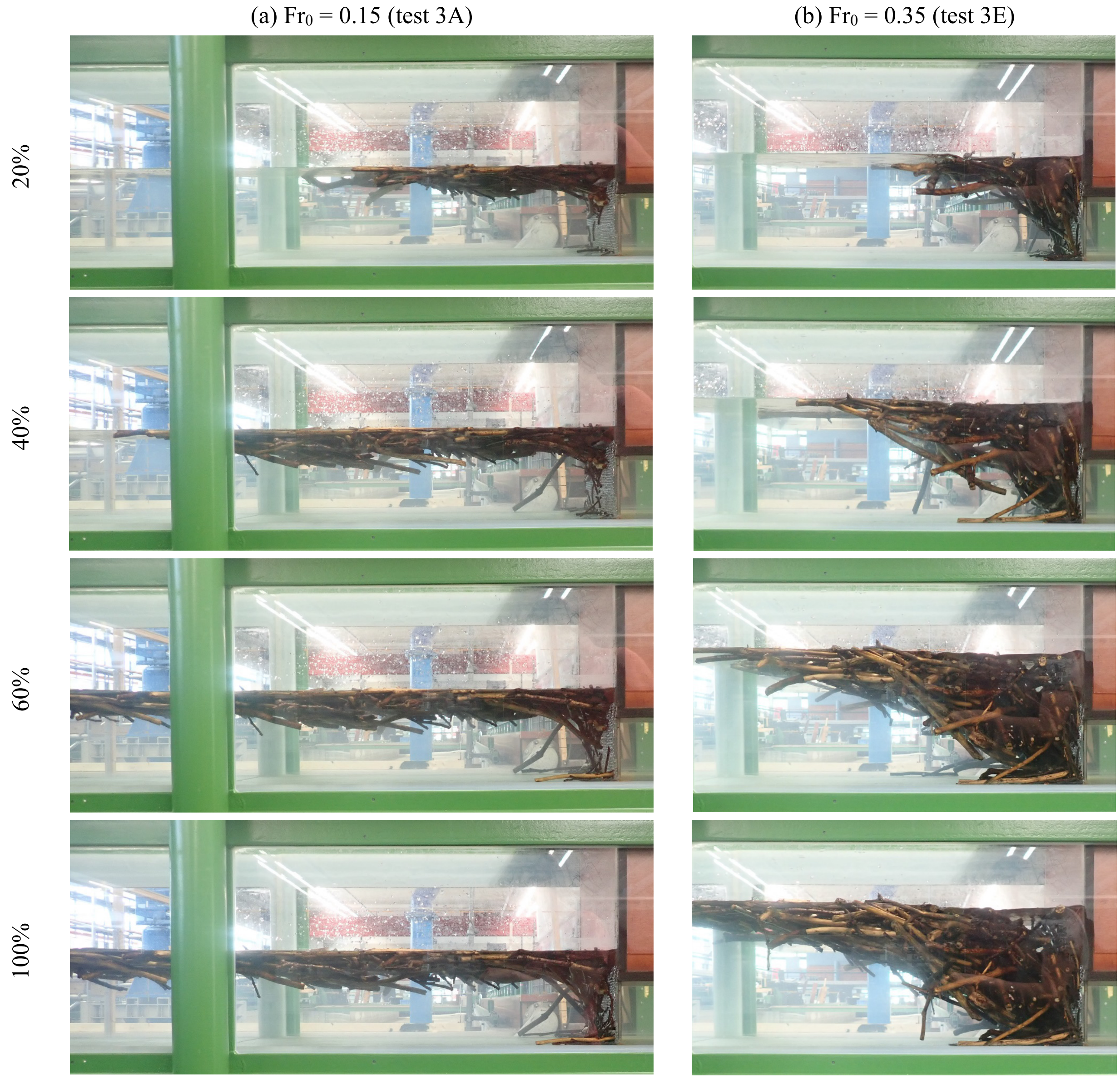

Figure 4. Evolution of driftwood accumulation for fraction of the total volumes for two selected flow conditions, both with an initial submergence h_0/δ = 1.4: (a) Fr_0 = 0.15 (test 3A); (b) Fr_0 = 0.35 (test 3E).

A relationship between the accumulation and the initial flow conditions is attempted in Figure 5, in the form

$$L_A = \beta \cdot \frac{V_S}{u_0^{\gamma}} \tag{1}$$

where β and γ are empirical parameters derived with best-fit approach with laboratory data. While Eq. (1) remains indicative, good agreement was observed for all volumes and initial flow conditions, with $\beta = 66.9$ and $\gamma = 0.74$ for variable L_A in meters, V_S in m^3 and u_0 in m/s.

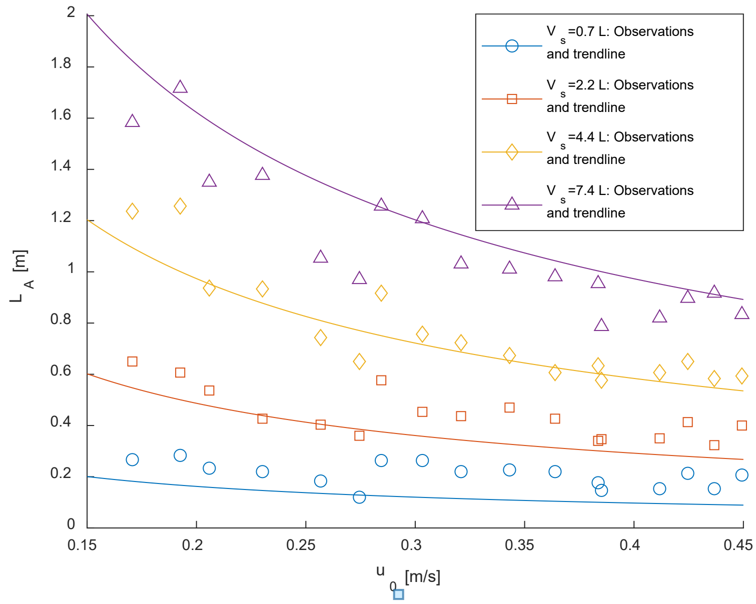

Figure 5. Observed carpet lengths, plotted for four driftwood volumes, decrease with increasing initial flow velocity. Fitted trendlines are of the shape $L_A = \beta \cdot \frac{V_S}{u_0^{\gamma}}$ in Eq. (1) with $\beta = 66.9$ and $\gamma = 0.74$.

For three flow conditions (Fr_0 = 0.15, 0.25 and 0.35; submergence 1.4), the thickness of the accumulation was measured every 5 cm in streamwise direction, with additional measurements near the inlet. By comparing the outer volume V_l to the solids volume fraction V_S the porosity of the accumulation can be estimated as $p = 1 - V_S / V_l$ as detailed in Table 2. Another way to express the ratio between outer volume and solid volume is the bulk factor a, defined as V_l / V_S. These are summarised in Table 2, showing that the accumulation porosity hardly changes with Froude number in these ranges that are defined by an outlet-controlled flow. Schalko et al. (2019a) found that the bulk factor for accumulations at pile structures can generally be approximated by $a = 5 - 1.35 \cdot Fr_0$ for Fr_0 between 0.3 and 1.5. In the case of $Fr_0 = 0.35$ this would amount to $a = 4.53$, which is similar to $a = 4.45$ found in the present experiments. Schalko et al. (2019a) also conclude based on a literature review that in real floods a is generally between 2 for dense accumulations and 5 for loose accumulations, which is in line with the values in Table 2 and therefore applicable to lower Froude numbers and for accumulations occurring at the inlet of submerged culverts.

Table 2. Porosity and bulk factor a of the three analyzed accumulations. The equation by Schalko et al. (2019a) is valid for Fr_0 between 0.3 and 1.5; $Fr_0 = 0.15$ and $Fr_0 = 0.25$ are outside of this range and slightly deviate from the measured values.

	$Fr_0 = 0.15$	$Fr_0 = 0.25$	$Fr_0 = 0.35$
Porosity $p = 1 - V_S / V_l$ [-]	75.9%	77.4%	77.5%
Bulk factor a [-] (measured)	4.15	4.43	4.45
Bulk factor a [-] (Schalko et al., 2019a)	4.80	4.66	4.53

4. VELOCITY MEASUREMENTS BELOW THE ACCUMULATION

For three selected flow conditions, detailed velocity profiles were measures using the LDA, as detailed in Section 2.1. At every point data was sampled for three minutes at a frequency of 1000 Hz. These measurements provided detailed information on the 2D flow field under the accumulation. An example of the time-averaged velocities is shown in Figure 6 for $Fr_0 = 0.35$ and a submergence rate of 1.4. Similar results were also obtained for $Fr_0 = 0.15$ and $Fr_0 = 0.25$, as detailed by Ronckers (2023a). Results show that horizontal velocities and velocity magnitudes decrease directly under the accumulation compared to lower in the water column. This is especially the case for the measurements at x = -36 cm (i.e. -3δ) and -24 cm (-2δ), which are sheltered by an upstream part of the accumulation extending further down. Near the start of the accumulation, at x = -60 cm (-5δ), a clear downward deflection of the flow is visible directly under the accumulation. Weaker downward flow is visible at the other measurement locations, which is a consequence of flow deflection by the accumulation and by the culvert opening being located near the bottom of the flume.

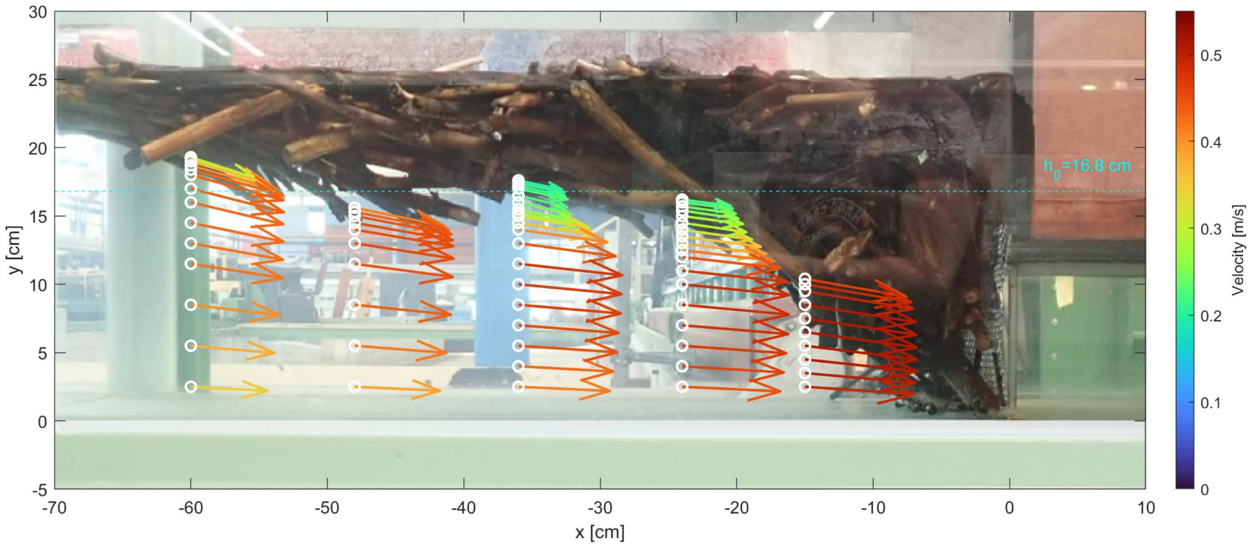

Figure 6. The velocity field under the accumulation, for $Fr_0 = 0.35$ and an initial submergence rate of 1.4. Average velocities are in the centre line of the flume, measured by the LDA.

Velocity profiles are plotted in detail in Figure 7, for the situation with and without driftwood, as well as profiles of the Reynolds stresses. At all depths, the horizontal flow velocities under the driftwood accumulation are lower than at the same position without driftwood, while vertical velocities are usually higher, especially directly under the accumulation. The horizontal velocities under the accumulation increase slightly in the *x*-direction, since the flow is funneled in the diminishing area underneath the accumulation, but they remain lower than the driftwood without driftwood until $x = -15$ cm (i.e. -1.25δ).

This means that the downward flow deflection by the driftwood is compensated by the cross-sectional increase from backwater rise. In fact, Figure 6 shows that the accumulation is located above the initial water level until approximately $x = -25$ cm ($x/\delta \sim -2$), resulting in little flow resistance within the original flow area and some '*additional*' weak flow on top of it, overall resulting in reduced velocities underneath the accumulation. This is remarkable, since accumulations at bridges and debris racks are reported to cause higher velocities near the bed, responsible for scour (Diehl, 1997; Schalko et al., 2019b). Although the lowest 25 mm could not be measured in our case due to limitations of the setup, significant flow acceleration at the bed seems unlikely from extrapolating the profiles. Possibly, flow acceleration only occurs when accumulations extend further down, whether that is at completely different accumulations and conditions, or simply elsewhere at the present accumulation (e.g. $x = -5$ cm in Fig. 6). Alternatively, it could be due to type of structure: the flow depth inside the pressurized culvert studied here cannot increase with backwater rise, like it would at more commonly studied bridges and debris racks. This fixed flow depth could result in higher backwater rise, increasing upstream flow depth and thus decreasing the probability of net flow acceleration.

Then Reynolds decomposition was applied to separate flow fluctuations from the mean flow values:

$$u_x = \bar{u}_x + u'_x \qquad\qquad u_y = \bar{u}_y + u'_y \tag{2}$$

where $\bar{u}_x$ and $\bar{u}_y$ are the time-averaged velocities and u'_x and u'_y the fluctuations. The Reynolds stresses were obtained from these turbulent fluctuations. Using u'_x and u'_y the normal stresses q_{xx} and q_{yy} as well as the shear stress $s_{xy} = s_{yx}$ were determined as

$$q_{xx} = \rho\, \overline{u'_x u'_x} \qquad\qquad q_{yy} = \rho\, \overline{u'_y u'_y} \qquad\qquad s_{xy} = \rho\, \overline{u'_x u'_y} \tag{3}$$

Looking at the behavior of these Reynolds stresses in Figure 7, the horizontal, vertical and shear stresses all show a sharp increase directly under the accumulation. This is especially apparent where there are large vertical gradients in the horizontal velocity profile, e.g. at $x/\delta = -5$ near the accumulation, or at $x/\delta = -3$, $y/\delta = 1.25$. These increased stresses can be explained by the rough bottom of the accumulation and the turbulent flow around logs. At $x/\delta = -2$ and $x/\delta = -3$, the highest measured locations show a clear drop in the stresses. These are the locations identified above as being sheltered by upstream driftwood (Figure 6). Conversely, the Reynolds stresses decreased compared to the situation without driftwood at the lowest data points. This effect was also observed when $Fr_0 = 0.25$, but in case of $Fr_0 = 0.15$ the difference in the lower half of the water column compared to the situation without driftwood was minimal.

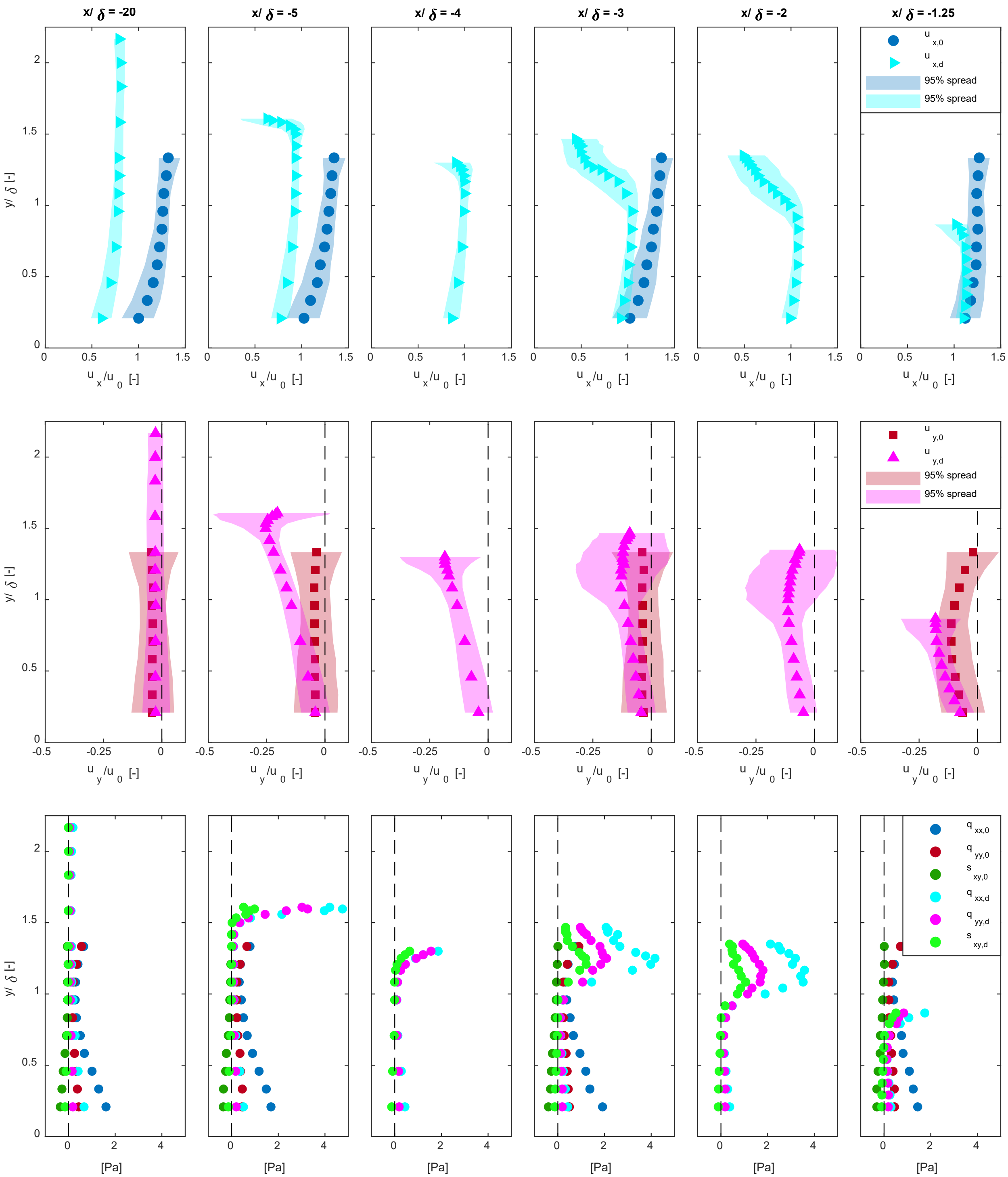

Figure 7. Measured horizontal velocities (top row), vertical velocities (middle row) and Reynolds stresses (bottom row) measured under the accumulation. Negative vertical velocity indicates downward flow. Markers indicate the value averaged over the 3 minute measurement intervals, shaded areas the 2.5th to 97.5th percentile, *i.e.* the 95% spread. Fr_0=0.35, h_0/δ=1.4, test 3E.

The velocity profiles measured underneath the accumulation allow to estimate the discharge that went through the accumulation Q_a. This is done by integrating the streamwise velocity profiles in Figure 7a assuming a typical logarithmic profile with u^* ~0.015 m/s, and a maximum roughness k_s ~1 mm. For maximum reliability, data was also corrected based on measurements without driftwood to take into account that flow velocities in the center of the flume are higher than near the sidewalls. This quantified the measured discharge below the accumulation Q_m while the discharge through the accumulation Q_a can be obtained as the difference between the total (measured) discharge and the discharge below the accumulation $Q_a = Q - Q_m$. Furthermore, the discharge through the accumulation Q_a has to pass through a cross-section of $B \cdot d$, where B is channel width and d is the depth of the accumulation at the location where the profile was measured. This gives an averaged velocity

$$u_{x,a,\mathrm{avg}} = \frac{Q_a}{B \cdot d} \tag{4}$$

The actual flow velocity through the pores of the accumulation, is the average velocity from Eq. (4) divided by the porosity p, which were found to be around 77.5%, as previous detailed in Table 2.

$$u_{x,a,\mathrm{pores}} = \frac{u_{x,a,\mathrm{avg}}}{p} = \frac{Q_a}{B \cdot d \cdot p} \tag{5}$$

The values of these average velocities through the accumulation $u_{x,a,avg}$ and $u_{x,a,pores}$ are plotted in Figure 8 together with the velocity profiles measured with the LDA, showing a relatively good agreement. In line with expectations, due to the increased friction, the velocities through the pores are lower than the velocities below the driftwood accumulation. However, the accumulation was highly non-uniform across the width of the cross section, suggesting that the velocities measured at the centerline might not be not representative of whole cross-section. Despite these limitations, these are promising results that will certainly contribute to a better understanding of the hydro-dynamic processes associated with the accumulation of driftwood at hydraulic structures.

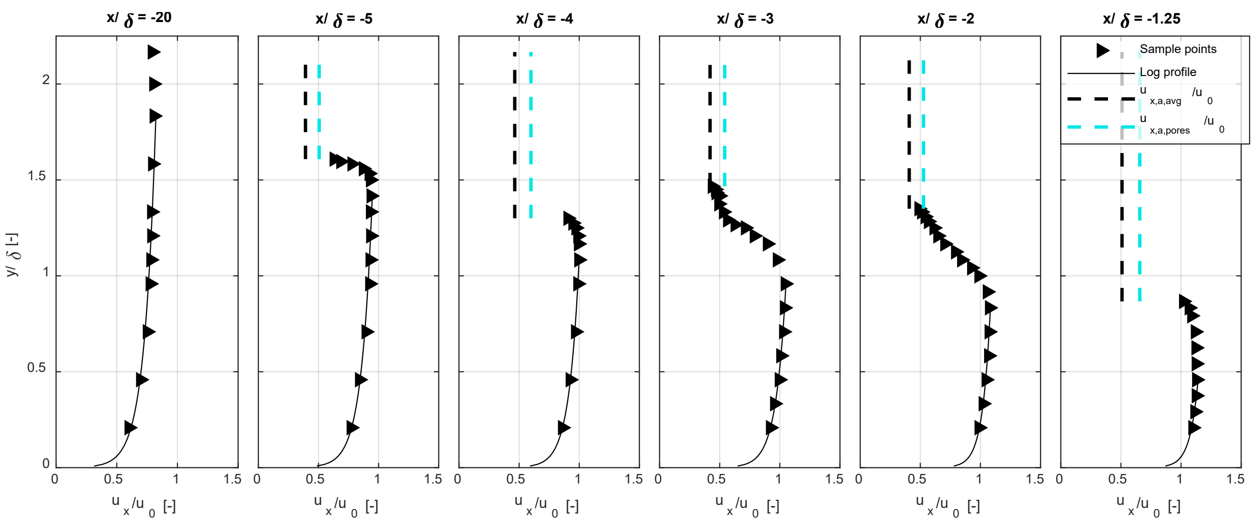

Figure 8. Flow velocities measured under the accumulation (same data presented in Figure 7a), together with the calculated flow velocities through the accumulation $u_{x,a,avg}$ and $u_{x,a,pores}$ defined in Eq. (4) and (5) respectively. ($Fr_0 = 0.35$, $h_0/\delta = 1.4$, test 3E).

5. CONCLUSION

In this study, scale experiments were conducted on driftwood accumulation at submerged culverts. Results of these experiments provided valuable insights into the accumulation process. The measured temporal evolution of the large wood accumulation and detailed velocity measurements offer a deeper understanding of the importance of large wood volume, accumulation geometry and hydraulic conditions for the build-up of accumulations and associated head-losses. The accumulation shape was found to depend strongly on the hydraulic conditions, with higher Froude numbers creating more compact accumulations with more logs pulled down toward the bottom, compared to lower Froude numbers creating a long floating carpet of logs at the water surface. While this accumulation shape effect in general is not new, it has larger consequences for the submerged culverts studied here, as the culvert opening near the bottom implies that flow resistance near the surface is of less importance than deeper in the water column. Quantitatively, the accumulation lengths in this study could be predicted well using the wood volume and initial flow velocity. In addition, measured backwater rise provides valuable data for the future, to help developing quantitative design equations for backwater rise from driftwood accumulation at submerged culverts. Lastly, velocity profiles and Reynolds stresses underneath the accumulations were measured in detail. This did not only show the flow field under the accumulation, but also, crucially, that the observed flow under the accumulation had a slightly *lower* velocity than without accumulation. Future research is needed to establish whether this is a generic trend of driftwood accumulation at submerged culverts – pointing to a lower likelihood of driftwood-induced scour – of if this is purely the result of the specific conditions and accumulations observed in this study.

ACKNOWLEDGMENTS

The project was funded through the Climate Action Program Seed Funds of Delft University of Technology. The authors would like to thank Prof. dr. ir. Wim Uijttewaal (Delft University of Technology, the Netherlands) for the helpful discussions and Ir. Chit Yan Toe for the support while using the LDA. The assistance of the technicians of the Hydraulic Laboratory of TU Delft is also gratefully acknowledged.

REFERENCES

Bayón, A., Valero, D., and Franca, M. J. (2024). Urban Flood Drifters (UFDs): identification, classification and characterisation. *ArXiv*. (preprint, under review).

Burghardt, L., Poppema, D.W., Bennet, L., Wüthrich, D., Erpicum, S., and Klopries, E.M. (2024). Multi-lab investigation of the effect of debris composition on the bridge clogging during floods. *Proceedings of the 10th International Symposium on Hydraulic Structures*, 17-19 June 2024, Zurich, Switzerland.

Diehl, T. H. (1997). *Potential drift accumulation at bridges* (Report nr FHWA-RD-97-028). US Department of Transportation: Federal Highway Administration.

Erpicum, S., L. Burghardt, D. W. Poppema, D. Wüthrich, E. Klopries, and L. Benet. 2023. *Deliverable D.T4.1.1 - Data collection, modelling and prediction* <https://emfloodresilience.eu/projects/work-package-4/>.

Follett, E., Schalko, I. and Nepf, H., (2020). "Momentum and energy predict the backwater rise generated by a large wood jam." *Geophysical Research Letters*, 47(17), e2020GL089346.

Fu, H., Guo, X., Kashani, A.H., & Wu, P. (2020). Experimental study of real ice accumulation on channel hydraulics upstream of inverted siphons. *Cold Regions Science and Technology*, 176.

Honingh, D., Van Emmerik, T., Uijttewaal, W., Kardhana, H., Hoes, O., & Van de Giesen, N. (2020). Urban River Water Level Increase Through Plastic Waste Accumulation at a Rack Structure. *Frontiers in Earth Science*, 8.

Korswagen, P. A., Harish, S., Oetjen, J., & Wüthrich, D. (2022). Post-flood field survey of the Ahr Valley (Germany): building damages and hydraulic aspects. *Delft University of Technology*.

Poppema, D.W. and Wüthrich, D., (2024). "Comment on 'Momentum and energy predict the backwater rise generated by a large wood jam'." *Geophysical Research Letters*. (accepted for publication)

Ronckers, D. (2023a). "*Effects of driftwood on backwater rise at submerged culverts*." *MSc Thesis*, Delft University of Technology, 67 pages.

Ronckers, D. (2023b). "*Hydraulic behaviour of the Geul inverted siphon: energy losses, debris accumulation and applicability of a Minimum Energy Loss culvert*." *Additional Thesis*, Delft University of Technology.

Ruiz-Villanueva, V., Stoffel, M., Piégay, H., Gaertner, V., & Perret, F. (2014). Wood density assessment to improve understanding of large wood buoyancy in rivers. *Proceedings of the International Conference on Fluvial Hydraulics*, 2014, 2503-2508.

Schalko, I. (2018). Modeling Hazards Related to Large Wood in Rivers. *PhD Thesis*, ETH Zürich, Switzerland.

Schalko, I., Lageder, C., Schmoker, L., Weitbrecht, V., & Boes, R.M. (2019a). Laboratory flume experiments on the formation of spanwise large wood accumulations: Part I – Effect on backwater rise. *Water Resources Research*, 55(5), 4854-4870.

Schalko, I., Lageder, C., Schmocker, L., Weitbrecht, V., & Boes, R.M. (2019b). Laboratory flume experiments on the formation of spanwise large wood accumulations: Part II – Effect on local scour. *Water Resources Research*, 55(6), 4871-4885.

Schmocker, L., and Hager, W.H. (2013). "Scale Modeling of Wooden Debris Accumulation at a Debris Rack." *Journal of Hydraulic Engineering*, 139(8), 827–836.

Wüthrich, D., Ylla Arbós, C. Y., Pfister, M., & Schleiss, A. J. (2020). Effect of Debris Damming on Wave-Induced Hydrodynamic Loads against Free-Standing Buildings with Openings. *Journal of Waterway, Port, Coastal, and Ocean Engineering*, 146(1), 04019036.